CONJUGATE HEAT TRANSFER ANALYSIS OF AN INTERNALLY COOLED TURBINE BLADES WITH AN OBJECT ORIENTED CFD CODE

CONJUGATE HEAT TRANSFER ANALYSIS OF AN INTERNALLY COOLED TURBINE BLADE WITH AN OBJECT ORIENTED CFD CODE

*B. Facchini – C. Bianchini – L. Mangani**

Dipartimento di Energetica "Sergio Stecco" Via Santa Marta, 3 - 50139 Firenze ITALY (*)

Email: luca.mangani@htc.de.unifi.it, WWW: http://www.htc.de.unifi.it

ABSTRACT

This paper presents the developments done on a CFD unstructured solver, based on OpenFOAM® CFD libraries, to perform conjugate heat transfer simulations. Such libraries permit polyhedral meshing and are based on a finite volume cell centered approach with both implicit and explicit discretization of differential operators. The solver uses a SIMPLE-like algorithm with a special treatment for the pressure corrector equation to deal with highly compressible flows.

To speed up convergence of the conjugate temperature equation a fully implicit approach has been adopted to solve the coupling for energy between solid and fluid region. Moreover an implicit treatment of generic interface has been developed and applied in this test, allowing treatment of non conformal cyclic patches.

The validation case to be shown is a subsonic test over the NASA C3X blade, cooled with ten internal ducts. Numerical and experimental results are compared in terms of pressure and temperature distribution on the blade wall at midspan, as well as heat transfer coefficient profiles. The mesh is a 1.3 million hybrid hexahedral, in the fluid, tetrahedral, in the solid domain.

NOMENCLATURE

Ch_A	axial chord	[m]
c_p	constant pressure specific heat	[J/(kg·K)]
c_ρ	compressibility	[s^2/m]
FV	finite volume	[-]
H	RHS Momentum equation	[kg/(m^2s)]
HTC	heat transfer coefficient	[W/(m^2·K)]
HTC_0	reference HTC value = 1135	[W/(m^2·K)]
k	thermal conductivity	[W/(m·K)]
L_d	turbulence dissipation length	[m]
p’	pressure corrector	[Pa]
phi	convective fluxes	[kg/s]
P.S.	pressure side	
PS_c	static pressure on cooling outlet	[kPa]
PS_{out}	static pressure on main outlet	[Pa]
PS_w	static pressure on blade wall	[Pa]
PT_{in}	total pressure on main inlet	[Pa]
$\dot{Q}$	wall heat flux	[W/m^2]
S.S.	suction side	
T	static temperature	[K]
T_{ref}	reference temperature = 811	[K]
T_{Sc}	static temperature on cooling inlet	[K]

TS_w	static temperature blade wall	[K]
TT_{in}	total temperature on main inlet	[K]
Tu	turbulence intensity	[-]
x	axial distance from leading edge	[m]
y	dimensional wall distance	[m]
y+	non dimensional wall distance	[-]

GREEK SYMBOLS

μ	dynamic molecular viscosity	[Pa·s]
μ_t	turbulent viscosity	[Pa·s]

SUBSCRIPTS

w	wall	[-]
s	solid	[-]
f	fluid, face	[-]
g	ghost	[-]
n	neighbor cell	[-]
p	interface internal cell	[-]

INTRODUCTION

Nowadays gas turbine engine temperatures in the first stage are well above those allowed by blade materials. Moreover, the persistent trend towards further enhancing efficiency and specific power has pushed up first vane inlet temperature as well as overall pressure ratio. Both constraints results in more severe operating conditions: the bigger the overall pressure ratio is, the higher is the compressor discharge temperature, i.e. the temperature of air available for cooling, see Han *et al.* 2000 .

For maintaining integrity of high pressure stage airfoils, cooling techniques need to be used: they commonly consist of internal passages of various shapes (fed by air bled from last compressor stages) coupled with a massive use of film cooling.

Computational Fluid Dynamics (CFD) has matured during recent years as a good predictive tool for gas turbine thermal design and analysis. The present industrial procedure to compute working temperature distribution of an airfoil typically develops in the following steps, see Carcasci *et al.* 2002: 1) treating two separate problems to determine both external and internal convective Heat Transfer Coefficient (HTC), 2) passing these results as boundary conditions to a finite element code and solving for conduction within the metal.

However, as long as flow and solid temperature calculations are kept uncoupled from each other, one may need several iterative processes to improve solution accuracy, since both internal and external HTC values depend on solid wall temperature. Solving instead for fluid and solid regions simultaneously, i.e. performing a Conjugate Heat Transfer (CHT) simulation, offers various advantages. In particular it should yield more realistic results in terms of heat transfer rate and flow field when compared to a solution obtained with an imposed heat flux or an isothermal boundary

The current paper aims at confirming CFD CHT simulations as a viable tool in gas turbine design: however, while the benefits and the current trend on CHT based simulations is favorable in general (as evident from the previously discussed papers), specific and additional contribution of the present investigation is to warn the reader on the effect of correct transition prediction when evaluating metal temperature field on a first stage airfoil through a CHT analysis.

The present work deals with the same geometry analyzed by York *et al.* 2003: the testcase is described in detail in the experimental study of Hylton *et al*. 1983. Briefly, it consists of the NASA-C3X linear cascade which has ten radial cooling channels almost located along the chamber line: the experimental activity conducted by Hylton *et al.* 1983. focused on measuring an accurate set of mid span data (pressure, solid temperature, and HTC profiles). These sets of data are used for

open-source CFD code validation purposes for heat transfer predictions after the addiction of specific modules.

According to that, a complete CHT simulation of NASA-C3X turbine vane has been performed using variants of the k-ε and k-ω Shear Stress Transport turbulence models. Detailed comparisons between experimental and numerical HTC, pressure, and solid temperature profiles are shown.

CODE DEVELOPMENT

This section describes the code developments applied to a frame of an open-source toolbox thought for continuum mechanics finite volume discretization, to produce fast and reliable heat transfer predictions of flows of turbo-machinery interest.

The development steps to make this code suitable for such simulations are described in order to point out its potentiality as a customizable CFD tool, appropriate for both academic and industrial research. The C++ library, named OpenFOAM® (Open-source Field Operation And Manipulation), offers specific class and polyhedral finite volume operators suitable for continuum mechanics simulations as well as built-in solvers and utilities. To make it robust, fast and reliable for RANS heat transfer predictions it was indeed necessary to implement additional submodules. The package coded by the authors within the environment includes a suitable algorithm for compressible steady-state analysis. A SIMPLE like algorithm was specifically developed to extend the operability field to a wider range of Mach numbers. A set of Low-Reynolds number eddy-viscosity turbulence models, chosen amongst the best performing in wall bounded flows, was developed.

After a first validation effort, see Mangani *et al.* 2007, Mangani *et al.* 2008 and Innocenti *et al.* 2008, based on internal thermo-aerodynamic, this article presents an attempt to enhance external aero-thermal prediction capability. Several issues still remain to be addressed within this task, especially in highly compressible regimes.

Numerical methods and physical modeling

The solver implements a SIMPLE like algorithm for steady-state flows modified to solve the Navier-Stokes equation in the compressible form. Extension to high Mach number flows requires the effects of density derivatives to be taken into account, thus introducing an extra convective term in the standard Fourier pressure equation which results from the mass continuity equation:

$$\nabla \cdot \left(c_{\rho} \cdot U \cdot p' \right) - \nabla \cdot \left(\rho \cdot H \cdot \nabla p' \right) = -\nabla \cdot \left(phi \right) \qquad (1)$$

With no possibility to implicitly relax such equation in order not to corrupt mass conservation, inlet boundary conditions become a major issue in solving such an equation. An inlet boundary condition to respect the total pressure constraint was implemented implicitly correcting mass imbalance in first cell layer to account for density variations at the boundary face.

Turbulence is taken into account in terms of RANS modeling with a wide selection of turbulence models specifically suited for heat transfer analysis. The option to test different turbulence models is crucial in case fluid nearwall behavior is of some interest. It is known for example that the choice of the turbulence model strongly influences heat transfer prediction, especially in proximity of recirculation zones, counter-pressure gradients, detached flows and many other effects quite common in turbo-machinery flows. Moreover heat transfer predictions along the blade are strongly dependent on inlet turbulence level. These are however a data that experiments often do not report with sufficient certainty. That is why a sensitivity analysis to the turbulence model and the inlet turbulence dissipation rate length scale was conducted in order to establish the most suitable values for such variable at the inlet.

In particular, due to the very detailed spatial discretization in the near wall region ($y^+ < 1$), it was possible to use Low-Reynolds number turbulence models such as the one-equation Spalart-Allmaras (SpAll in short), see Spalart *et al.* 1992, the two-layer k-ε (TL in short), see

Rodi 1991 also in the RNG form (TL-RNG in short), see Yakhot *et al.* 1992 and the k-ω SST (k-w in short), see Menter 1993. For further details on solver and turbulence models implemented refer to Mangani *et al.* 2007 and to Mangani *et al.* 2008.

Conjugate Heat Transfer Coupling

The energy equation for the two domains is written in same form (static temperature) and discretized in the same matrix. The full Navier-Stokes energy equation in fact reduces to the simpler conduction equation in case the fluxes are null as they are in the solid domain.

$$\nabla\ phi \cdot c_p \cdot T\ /\ A\ - \nabla\ k \nabla T\ = \nabla\ phi\ /\ rho \cdot A\ \cdot p\ - p \cdot \nabla\ phi\ /\ rho \cdot A\ \xrightarrow{phi=0} \nabla\ k \nabla T\ = 0 \quad (2)$$

In this manner the coupling between the two sides of the interfaces can be easily treated in an implicit way just discretizing the energy flux in terms of both solid and fluid adjacent cell thus respecting at each iteration both the continuity of temperature profiles and the equality of thermal fluxes across the interface. The coefficients of mutual interaction are directly calculated from the conservation of energy across the boundary face weighting temperature at cell center with conductivity and distance from the wall.

$$\frac{k_f}{\Delta y_f}\ T_f - T_w\ = -\frac{k_s}{\Delta y_s}\ T_s - T_w\ \Rightarrow T_w = \frac{\frac{k_f \cdot T_f}{\Delta y_f} + \frac{k_s \cdot T_s}{\Delta y_s}}{\frac{k_f}{\Delta y_f} + \frac{k_s}{\Delta y_s}} \Rightarrow$$

$$\nabla T_{ws} = \frac{1}{\Delta y_s} \underbrace{\left(1 - \left(\frac{\frac{k_s}{\Delta y_s}}{\frac{k_s}{\Delta y_s} + \frac{k_f}{\Delta y_f}} \right) \right)}_{Diag.Coeff.} \cdot T_s - \frac{1}{\Delta y_s} \underbrace{\left(\frac{\frac{k_f}{\Delta y_f}}{\frac{k_s}{\Delta y_s} + \frac{k_f}{\Delta y_f}} \right)}_{Extra-diag.Coeff.} T_f \quad (3)$$

This implicit technique allows faster convergence rates compared to standard explicit coupling used in other codes, due to the fact that energy balance is strictly respected at each iteration step, meaning that the temperature residuals in the solid only follow the implicit relaxation and not the update of the boundary conditions, basically not overloading non-conjugate calculations convergence rates. Parallelization is achieved decomposing the interface to maintain the two cells across the boundary face on the same processor. This special boundary condition can be applied only to a Low-Reynolds- number mesh on the fluid part because of a linear approximation can be considered valid in the thermal boundary layer only if the first fluid cell node is close enough to the wall. With such an assumption total and static temperature coincide close to the wall implying that this boundary condition can be extended also to total temperature equation.

Validation was performed on purely conductive tests as well as on a turbulent flat plate case (Xue 2005) with very good agreement with both correlative and theoretical results.

Generic Grid Interfaces GGI

In order to ease the mesh generation process, to allow a fully independent meshing of the different domains and to increase mesh quality in highly curved periodic interfaces a very general connection algorithm has been developed. Such an algorithm deals with multiple implicit coupling of unstructured mesh. A ghost cell is used to store the contributions of all the neighbor cells weighted on the face overlapping area. The ghost cell is updated at every iteration of the linear system solver therefore achieving pure implicit coupling between the two sides of the interface.

$$\phi_f = w_p \cdot \phi_p + \left(1 - w_p\right) \cdot \phi_g \Rightarrow \phi_g = \sum_n \alpha_n \phi_n \qquad (4)$$

A pre-processing tool is used to calculate and store both the addressing of the cells of mutual interaction and the weighting factors. Basically this tool calculates the overlapping area of the faces using an algorithm based on the definition of the winding number, valid for all polygons unless they are self-intersecting and have different orientation. If these two requirements are satisfied, and this is always the case if volumes of cells are positive, the integral of the product of the winding number of the two polygons is the intersection area. Obviously two polygons in space must be coplanar in order to share a finite portion of area, indeed this can be problematic in case of curved boundaries such as blade to blade periodic boundary. To prevent such failure of the algorithm the faces are first projected onto a common plane and so the projected overlapping areas are calculated. This does not invalidate the algorithm bearing in mind that the relative weight of the overlapping areas is actually the fundamental quantity to be calculated. If the overlapping area goes beyond a very tight tolerance the address of the cell is stored in the set of neighbor cells.

$$\alpha_n = \frac{A_{fn-fp}^{overlap}}{A_{fp}} = \frac{A_{fn-fp}^{overlap}{}_{projected}}{A_{fp}{}_{projected}} \qquad (5)$$

This coupling can be applied to both coincident interfaces as well as periodic boundaries like rotational or translational cyclic but at the moment such treatment is not implemented for fluid-solid interfaces. It works in parallel exploiting MPI communication, the send and receive mechanism is built up in order to include only the nodes actually sharing a GGI boundary thus not overloading any of the processors with collecting and sending tasks. Multiple definition of GGI is also possible inside the same domain.

CONJUGATE CALCULATIONS

Simulation Setup

The numerical model simulates experimental setup of Hylton *et al.* 1983: they performed detailed investigations on two aerothermodynamic linear cascade facilities. In particular NASA-C3X cascade was made up of three vanes representative of a gas turbine first stage. The center blade of the cascade was instrumented for heat transfer and aerodynamic measurements. Each stator was cooled by an array of 10 radial cooling holes: each hole of the test airfoil was fed by a metered line while those of the adjacent blades were supplied by a common plenum. A burner and a turbulence augmentation grid were present in the facility to control total temperature and turbulence intensity of the flow entering the vanes .

P_{Tin}	T_{Tin}	L_d	Tu	P_{Sout}
321800	783	5e-6	0.083	192500

Table 1: Boundary condition imposed for the external gas path.

N°	1	2	3	4	5	6	7	8	9	10
M	.0078	.0066	.0063	.0067	.0065	.0067	.0063	.0023	.0014	.0007
T_{Sc}	387	388	371	376	355	412	367	356	406	420
P_{Sc}	100	100	100	100	100	100	100	100	100	100
L_d	.001	.001	.001	.001	.001	.001	.001	.001	.001	.001
Tu	.05	.05	.05	.05	.05	.05	.05	.05	.05	.05

Table 2: Boundary conditions imposed for the internal cooling channels

Following data were stored for each experimental test: Reynolds number and mass averaged static temperature of every single cooling channel in the test airfoil; turbulence intensity, total pressure and total temperature of the fluid entering the cascade; static pressure at cascade outlet; mid span profiles of both static pressure and temperature on test vane surface. Acquired data were then passed to a dedicated code for solving conduction within the airfoil and the HTC mid span distributions were determined for each case.

In order to save CPU memory and computational time, periodic boundaries are used in the numerical model (Figure 1). According to the conjugate nature of the simulation, boundary conditions are imposed only on the openings of the computational domain: a fixed mass flow rate and a constant static temperature were set in the inlet of each cooling channel, constant static pressure was imposed both in the main and in the cooling channel outlets, uniform total pressure and total temperature were assigned in the main inlet. Hub and tip walls were modeled as adiabatic and no slip conditions were applied. Furthermore, as required by the two-equation turbulence models used, Tu and L_d have been fixed at every inlet.

Tables 1 and 2 summarize all above conditions for a particular case reported by Hylton *et al.* 1983 (code N° 4422, run N° 112). Definitive values of static inlet temperatures imposed on cooling channel inlets were found via an iterative process aimed at matching, for each channel, experimental mass averaged static temperature.

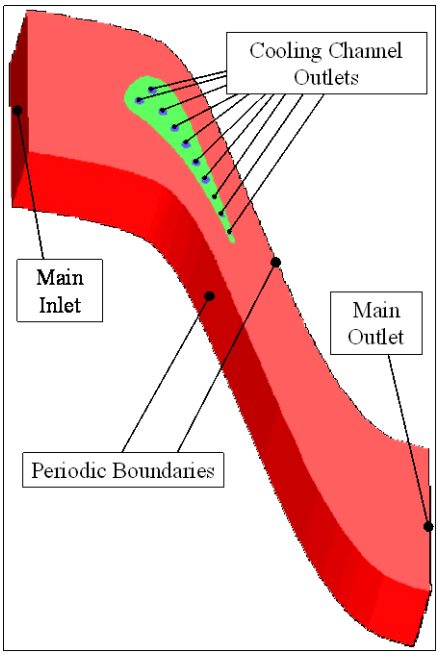

Figure 1: Computational domain and boundary conditions used.

The mean flow satisfies the Reynolds Averaged Navier-Stokes (RANS) equations together with perfect gas law (molecular weight is 28.96 [kg/kmol]). Thermophysical properties were set up imposing calorically perfect behavior with constant pressure specific heat capacity c_p = 1075 [J/(kg·K)], dynamic viscosity μ = 3.33e-05 [kg/(m·s)] and Prandtl number Pr = 0.684.

The specific heat capacity of vane material (310 stainless steel) is set constant to 473 [J/(kg·K)] and, based on experimental data (Goldsmith *et al.* 1961), the thermal conductivity was specified to vary linearly with temperature: $\lambda_b(T) = 6.811 + 0.020176 \cdot T$.

Computational mesh

In Figure 2 the computational grid used for conjugate calculations is shown. It consists of three different parts: an unstructured mesh for the solid vane domain, and two multi block structured grids for calculation of external gas path and internal cooling flow field.

Mesh dimension of the external part is about 700000 FV. An O-type mesh is present close to the airfoil to ensure orthogonal grid clustering at wall and properly resolve viscous sublayer: y^+ value remains below 0.5 on all the blade profile. Grid clustering is also applied behind the blade trailing edge to capture airfoil wake.

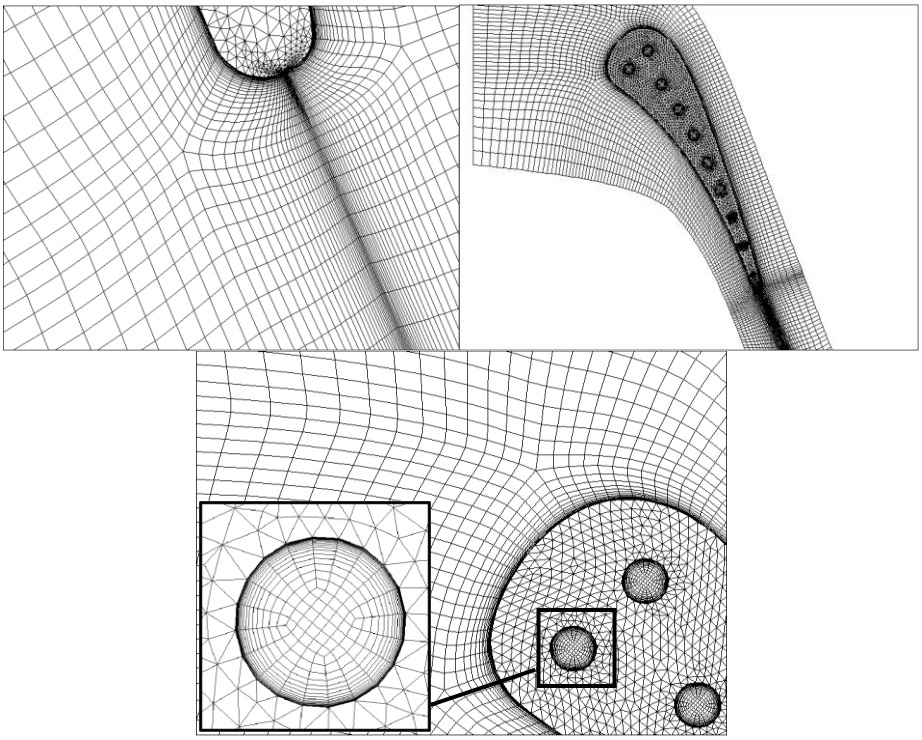

Figure 2: Mesh used for conjugate calculations.

As confirmed by Figure 2, subdivision of external domain in 15 blocks led to very low skewness of grid volumes, every internal angle of the generic volume being comprised between about 72 and 108 degrees. Unstructured solid part size is about 190000 FV: according to the physics of the conductive problem no refinement is present in proximity of blade surfaces. Internal part grid size is about 280000 FV and near wall layer thickness of each channel is such to ensure everywhere a maximum y^+ of about 0.5.

ANALYSIS OF RESULTS

Flow field predictions

In order to establish and validate the correct implementation of the newly introduced feature, namely the Generic Grid Interface algorithm, at first non-conjugate two-dimensional case at a fixed wall temperature was performed reproducing the already described set-up in terms of vane flow field. Continuity and smoothness of contour lines were checked across the cyclic interface together with the global conservation of mass. The non conformal periodic fluid-to-fluid interface strictly conserves mass, reducing imbalance up to the geometrical error induced by geometrical discretization. Such geometrical error is indeed not null only in case of non planar interfaces, in the case to be shown for example the relative difference in the sum of face areas is in the order of 1e-4 between the two sides of the interface. The smoothness of pressure contour plots across the interface can be appreciated in Figure 4.

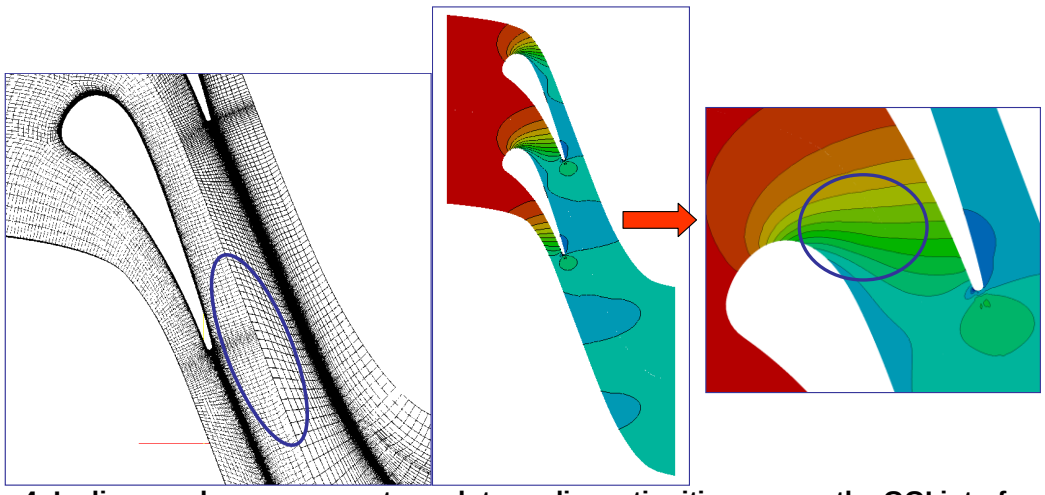

Figure 4: Isolines and pressure contour plot: no discontinuities across the GGI interface .

Regarding the three dimensional calculation blade load predictions are tested against both experimental and numerical results obtained with the commercial CFD code STAR-CD v3.15 with the two-layer k-ε turbulence model, in a similar configuration, see Facchini *et al.* 2004. In particular non-dimensional pressure contour at mid span was available to compare the different models' behaviour.

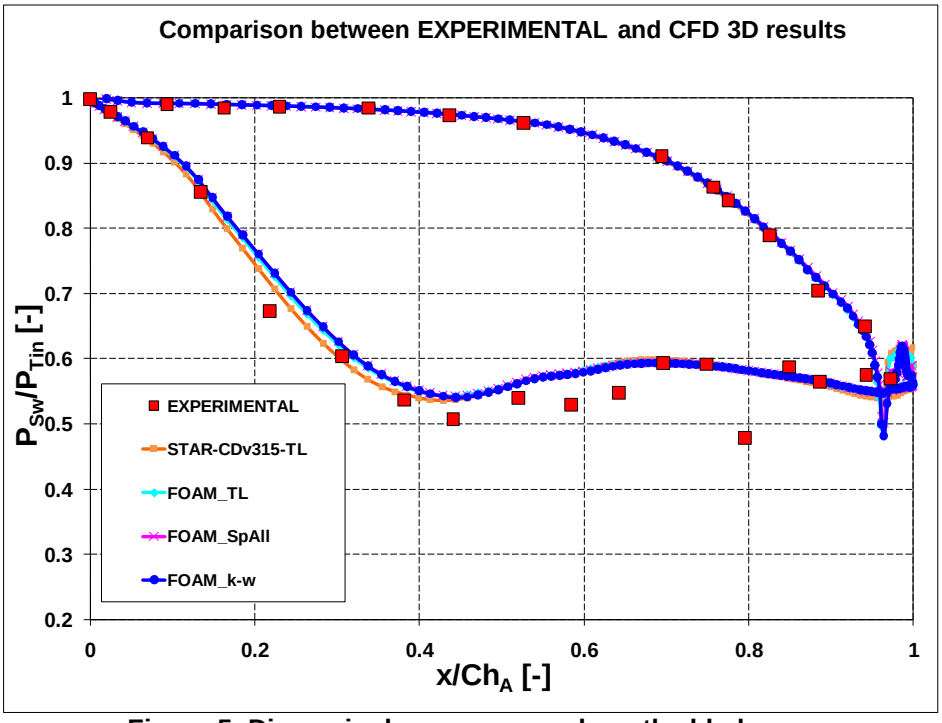

Figure 5: Dimensionless pressure along the blade.

As it is shown in Figure 5 the dependency of blade load on turbulence model is quite low and all models show a general good level of agreement with the experimental data, practically confining the only critical zone in the first half of the suction side where the highest pressure gradients are located. This can be ascribed to the excessive turbulent kinetic energy production around the leading edge which deeply affects viscous loss mechanism thus resulting in a weaker acceleration around the nose. Star-CD predictions in fact, due to a realizability constraint that limit turbulent kinetic energy production do not show such behavior.

Heat transfer predictions

Even though previous section showed how pressure load is almost insensitive to turbulence modeling and the level of agreement obtained with experimental results is quite high, this cannot be considered true for heat transfer predictions. Due to the thin thermal boundary layer and the importance of the wall temperature gradient, good aerodynamic predictions are not sufficient to guarantee correct predictions of heat transfer phenomena. Usually this lack is attributed to boundary condition uncertainty and difficulty in finding a suitable turbulence closure: that is why several turbulence models were tested at the same conditions. The experimental results to match with are reported in terms of non-dimensional wall temperature, moreover such temperature distribution was used to extract via an FEM solver a heat transfer coefficient profile.

As it may be noticed in Figure 6, the two-layer models do not predict a local maximum in the values for heat transfer coefficient, defined as $HTC = \dot{Q} / \left(TS_w - TT_{in} \right)$, at the leading edge but with a typical fully turbulent behavior increase heat exchange on the suction side. While for the standard model the HTC is overestimated along the entire profile, the ReNormalization Group variant, reducing the level of turbulence near the wall, results in line with experimental data both at leading edge and downstream on the suction side. Better matching can be obtained using k-ω SST and Spalart-Allmaras models.

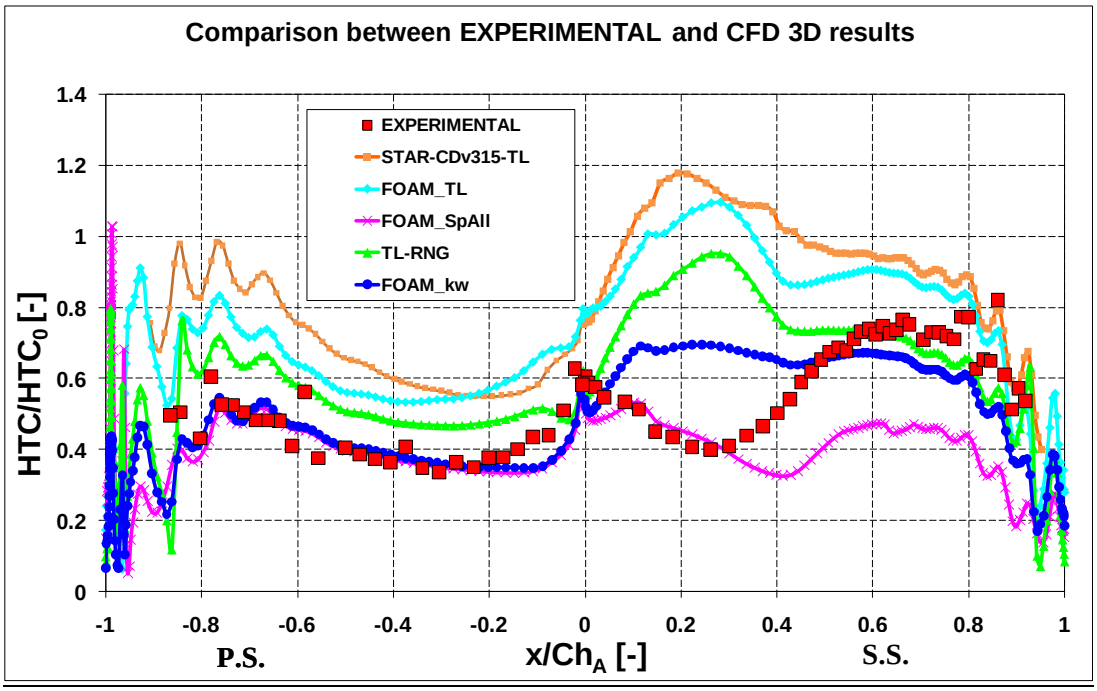

Figure 6: Dimensionless heat transfer coefficient profile at midspan.

Even though the two models seem to overlap on the pressure side with a very good agreement with the experimental investigation, the different nature of the two models is shown in the suction side. The k-ω SST in fact is following the turbulent trend to increase heat transfer coefficient downstream the leading edge but with a weaker level of enhancement compared to two-layer models. This however results in an underestimation of heat transfer coefficient for $x/Ch_a > 0.5$. On the contrary Spalart-Allmaras model correctly predict laminarization on the early suction side but it shifts the transition point downstream compared to experimental evidence. As a consequence the turbulent increase of HTC is not sufficient to rematch experimental curve close to the trailing edge. It is interesting to point out how the HTC growth rate after transition occurs is the same as in the experiments, this is well promising for further development of the code: correctly predicting transition point could really improve the global level of agreement.

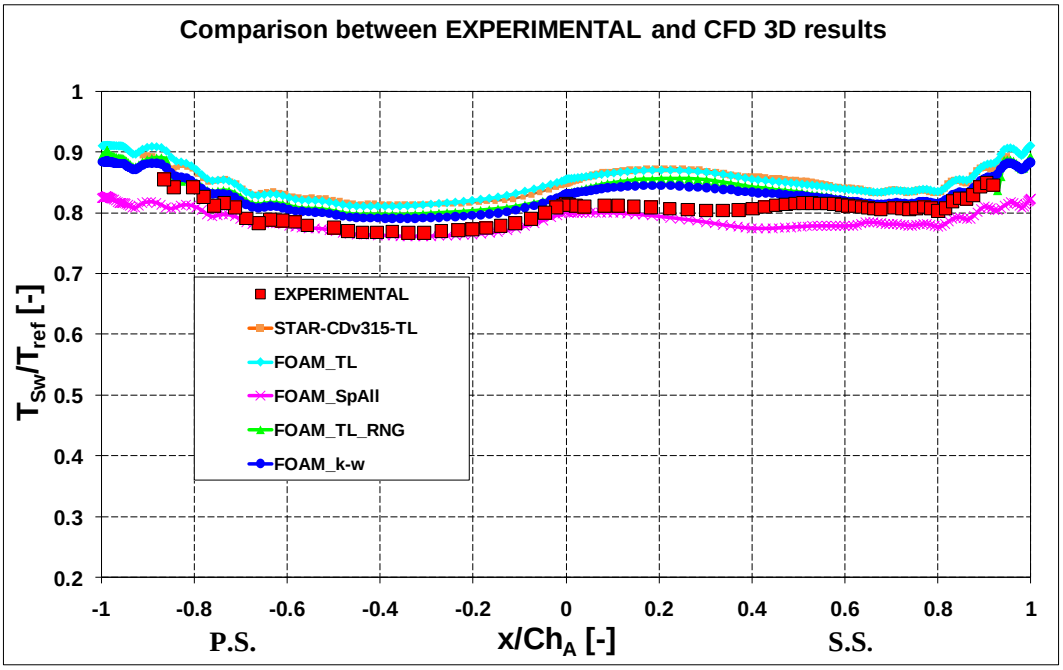

Figure 7: Dimensionless temperature profile at midspan.

Figure 7 shows the profiles of wall temperatures: the trends of the previous graph are confirmed, assessing the standard two-layer model, both Star-CD and OpenFOAM®, to higher levels of temperature, the k-ω SST and the two-layer RNG to an intermediate level and the Spalart-Allmaras a little bit in underestimation. The model that globally matches better experimental results is the Spalart-Allmaras with major misalignments downstream the suction side. The two intermediate models, basically shifts the standard two-layer profile up to values that matches estimated temperature near the trailing edge better on suction than on pressure side.

CONCLUSIONS

A turbulence model assessment and the adaptation of the OpenFOAM® C++ libraries for conjugate heat transfer of a turbine vane model have been performed.

OpenFOAM® has been improved to predict heat transfer phenomena in gas turbine blade cooling: in details Generic Grid Interfacing and implicit conjugate heat transfer module have been developed and validated. The object oriented language used is found to be very flexible for implementing new modules, algorithms and physical models.

The reference test case studied was based on the NASA-C3X linear cascade, cooled by ten radial channels representative of a gas turbine first stage and results were compared with measured data. Loading distributions were found to be in good agreement with experiments for all turbulence models. Good agreement with experimental measurements was found in terms of Heat Transfer Coefficient and wall temperature only for the Spalart-Allmaras and k-ω SST turbulence models, while two equation k-ε turbulence models both with the tested commercial and open source CFD code present large disagreements with respect to experiments.

For all the models used as evidenced by measurements, both pressure and suction side exhibit a typical transitional behavior. For this reason, HTC profiles obtained without taking into account transition severely overestimate experimental data, especially near the leading edge, where a laminar region is present: results can be improved with the development and the applications of specific transition models.

Finally, the modified version of the object oriented OpenFOAM® C++ libraries for continuum mechanics modified to handle CFD heat transfer in turbomachinery applications is a good and

efficient solution framework and it can be considered as a real alternative to the CFD commercial software.

Future work will be concentrated on expanding the capability of the code to simulate fluid-structure interaction with the new GGI boundaries between fluid and solid domains and to develop algorithms for the agglomeration in the Algebraic Multi Grid linear solvers specific for the GGI boundaries.

ACKNOWLEDGEMENTS

This work was conducted within a collaboration contract between the Energy Engineering Department of the University of Florence and the industrial partner ANSALDO Energia Spa.

REFERENCES

Carcasci, C., Zecchi, S., Oteri, G., "*Comparison of Blade Cooling Performance Using Alternative Fluids*", ASME paper GT-2002-30551, ASME Turbo Expo, June 2002.

Demelenuar *et al., "Application of an unstructured flow solver to the calculation of conjugate heat transfer problems in turbine blades",* European Turbomachinery Congress, 2005.

Goldsmith, A., Waterman, T. E., Hirshhorn, H. J., *Handbook of Thermophysical Properties of Solid Materials – Volume II: Alloys*, The Macmillian Company, 1961.

Facchini *et al., "Conjugate heat transfer simulation of a radially cooled gas turbine vane",* ASME paper GT2004-54213, ASME Turbo Expo, June 2004

Han, J., Dutta, S., Ekkad, S. V., "*Gas turbine Heat Transfer and Cooling Technology*", Taylor & Francis, 2000.

Hylton, L. D., Mihelc, M. S., Turner, E. R., Nealy, D. A., York, R. E., 1983, "*Analytical and Experimental Evaluation of the Heat Transfer Distribution Over Surfaces of Turbine Vanes*", NASA Technical Report, NASA-CR-168015.

Innocenti *et al., "Development of numerical tools for stator-rotor cavities calculation in heavy-duty gas turbines"*, ASME paper GT2008-51268, ASME Turbo Expo, June 2008.

Mangani *et al., "Development and validation of a C++ object oriented CFD code for heat transfer analysis"*, ASME paper AJ2007-1266, ASME-JSME Thermal Engineering and Summer Heat Transfer Conference, July 2007.

Mangani and Andreini, *"Application of an object-oriented CFD code to heat transfer analysis"*, ASME paper GT2008-51118, ASME Turbo Expo, June 2008.

Menter, *"Zonal two equation k−w turbulence models for aerodynamic flows"*, AIAA Paper 93-2906, 1993

Rodi, W., "*Experience with Two-Layer Models Combining the k-ε Model with a One-Equation Model near the Wall*", AIAA paper 91-0216, 1991.

Spalart, P. R. and Allmaras, S. R., "*A One-Equation Turbulence Model for Aerodynamic Flows*", AIAA Paper 92-0439, 1992

Xue, *"Development of conjugate heat transfer capability to an unstructured flow solver – U^2NCLE"*, Master thesis Mississipi State University, 2005.

Yakhot, V., Orszag, S.A., Thangam, S., Gatski, T.B., and Speziale, C.G., "*Development of Turbulence Models for Shear Flows by a Double Expansion Technique*", Phys. Fluids, 4, pp. 1510-1520, 1992.

York, W. D., Leylek, J. H., "*Three-Dimensional Conjugate Heat Transfer Simulation of an Internally-Cooled Gas Turbine Vane*", ASME paper GT2003-38551, ASME Turbo Expo, June 2003.